Nanostraw–Electroporation System for Highly Efficient Intracellular Delivery and Transfection

Xi Xie,[†] Alexander M. Xu,[†] Sergio Leal-Ortiz,[‡] Yuhong Cao,[†] Craig C. Garner,[‡] and Nicholas A. Melosh[†,*]

[†]Department of Materials Science and Engineering, Stanford University, Stanford, California 94305, United States and [‡]Department of Psychiatry and Behavioral Sciences, Stanford University, Stanford, California 94304, United States

ABSTRACT Nondestructive introduction of genes, proteins, and small molecules into mammalian cells with high efficiency is a challenging, yet critical, process. Here we demonstrate a simple nanoelectroporation platform to achieve highly efficient molecular delivery and high transfection yields with excellent uniformity and cell viability. The system is built on alumina nanostraws extending from a track-etched membrane, forming an array of hollow nanowires connected to an underlying microfluidic channel. Cellular engulfment of the nanostraws provides an intimate contact, significantly reducing the necessary electroporation voltage and increasing homogeneity over a large area. Biomolecule delivery is achieved by diffusion through the nanostraws and enhanced by electrophoresis during pulsing. The system was demonstrated to offer excellent spatial, temporal, and dose control for delivery, as well as providing high-yield cotransfection and sequential transfection.

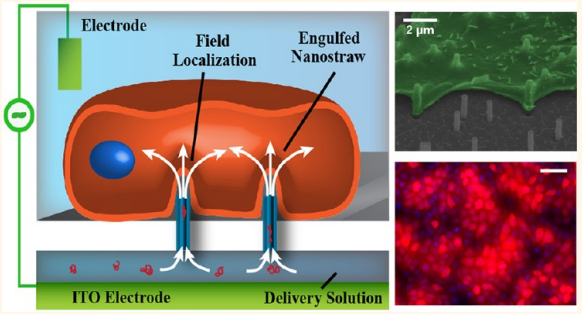

KEYWORDS: nanobiotechnology · electroporation · drug delivery · transfection · biointerfaces

Introduction of small molecules, proteins, and genetic material across the cell membrane with high efficiency is a challenging, yet critical, technique in biological and medical research.[1−4] Chemical (lipofectamine,[5] cationic polymers[6]) and biological reagents (cell penetrating peptides,[7] viral vectors[8]) are widely used to enhance material transport across cell membranes, yet these methods are often limited by the low efficiency of plasmid delivery into many cell types due to plasmid degradation or safety concerns.[1,3,9,10]

Rather than rely on biochemical processes and the accompanying endosomal degradation complications, more direct approaches to physically breach the cell membrane have been developed, the most common of which is electroporation. Transfection by electroporation relies on applied electrical fields to create transient holes in cell membranes and drive biomolecules into the cytosol.[11−15] While conventional bulk electroporation is suitable for the treatment of a large number of cells at once, it must be performed at high voltage with cells in suspension and requires a considerable quantity of reagents. High cell viability and uniform transfection are difficult to achieve because of inhomogeneities of the electric field across each particular cell.[9,16] Lee and co-workers have developed electroporation devices based on cells supported on porous membranes to improve the uniformity of the electric field across the cells.[17,18] These are performed by sandwiching the cells between two porous sheets and applying suction. However, nonuniform cell-to-substrate contact reduces the transfection yield for a given cell viability.[17,19]

Recently, significant progress has been made using nanomaterial platforms for intracellular delivery. Direct cell membrane penetration by small-diameter nanowires may serve as universal platforms for introducing biomolecules into a broad range of cell types, and can be performed in parallel for a large number of cells.[20−23] Yet, even in this case, the stochastic nature of cell penetration[24,25] and molecular elution from the nanomaterials complicate control over the temporal and dose of delivered biomolecules. We recently reported a nanostraw (hollow nanowire) platform that provides excellent time-resolved and spatially controlled intracellular access relying on the

* Address correspondence to nmelosh@stanford.edu.

Received for review February 20, 2013 and accepted April 18, 2013.

Published online April 18, 2013
10.1021/nn400874a

spontaneous penetration of small diameter (~100 nm) nanostraws into cells.[26] However, the DNA plasmid transfection efficiency is generally low (~10%). Moreover, the nanostraw–cytoplasm connection remains open after the penetration event. Although such stable fluidic interfaces are favorable in terms of temporal control of delivery, the biological behavior could be influenced due to protein and ion leakage through these channels.

Here we show a nanoelectroporation system for efficient intracellular delivery and transfection with high cell viability based on nanostraws (Figure 1a,b). Due to the close interface between the cell membrane and each nanostraw, the electric field is localized, inducing transient membrane permeability only over a small area. The uniform contact geometry also reduces the variability of the local voltage, so that a larger fraction of cells are porated at a particular voltage, with less cell death. Short duration (20–200 μs) electrical pulses with low voltage (5–20 V) can serve as a valve to open the cell membrane and drive biomolecules into the cytoplasm. Because the electroporated region is coincident with the reagents delivered from the nanostraws, this may increase the efficiency of biomolecules bypassing the porated cell membrane compared to conventional electroporation (Supporting Information, Figure S1).

Results from nanostraw electroporation show highly efficient dye delivery (>95%) and plasmid transfection (~81%) into Chinese hamster ovary cells (CHO), as well as Human Embryonic Kidney (HEK) 293T cells (plasmid transfection ~67%), all with high cell viability (>98%). In addition to spatial and temporal control, the system offers dose control, high-yield cotransfection (simultaneous transfection of two or more DNA plasmids) and sequential transfection (transfection of one or more types of DNA plasmids on different days). The versatility, efficiency, and uniformity of the nanostraw-electroporation system serve as a powerful and reliable platform for high-throughput intracellular delivery and transfection.

RESULTS

Nanostraws were fabricated as described previously.[26] Briefly, 20 nm thick aluminum oxide was deposited on all the surfaces of a track-etched polycarbonate membrane with atomic layer deposition (ALD). The top alumina layer was removed with a reactive ion etch, and the exposed polymer was selectively oxygen etched to reveal the alumina nanostraws (Supporting Information, Figure S2). Typical nanostraw has 250 nm diameters and 1.5 μm height (Figure 2a). These nanostraws show close contact with the cell membrane but were too large to spontaneously penetrate the cell.[26] Typical nanostraw number densities were 0.2 straws/μm^2, which is roughly 10–50 straws/cell for adhered CHO or HEK 293 cells (Figure 2b).

The electroporation device architecture is shown in Figure 1a. The nanostraw membrane is integrated between a polydimethylsiloxane (PDMS) microfluidic channel and a second PDMS layer with a cell culture well. Indium tin oxide (ITO)-coated glass underneath the microfluidic channel serves as the bottom electrode, and a Pt electrode placed in the cell culture well serves as the top electrode. As illustrated in Figure 1b, the electrical field is generated between the ITO coated glass and Pt electrode and passes through each nanostraw. Biomolecular delivery through nanostraws into electroporated cells is regulated by controlling the solution composition in the microfluidic channel. Biomolecular transport through the straws and across cell membranes is driven by diffusion and also the applied electric field during electroporation. Cells are cultured in a routine manner on top of the nanostraw membrane. CHO cells spread and proliferate on the nanostraws in similar fashion to cells on flat membranes, and engulf the nanostraws based on SEM imaging (Figure 2c,d).

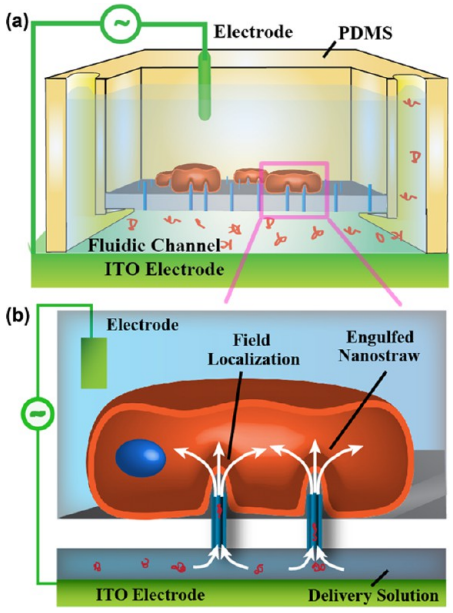

Figure 1. Illustrations of nanostraw-electroporation system. (a) Schematic view of device. (b) Schematic illustration of field localization and biomolecule confinement at the tip of the nanostraw due to close contact at the nanostraw–plasma membrane interface.

Experimentally, we evaluated whether propidium iodide (PI), a membrane-impermeable fluorescent DNA intercalator, or a plasmid (pRFP) encoding red fluorescent protein (RFP) would enter CHO cells by nanostraws-electroporation. Note, these molecules normally are unable to penetrate the plasma membrane and enter the cytosol without facilitating transport agents. In initial experiments, CHO cells were grown on the nanostraw membrane for 24 h and then examined whether electroporation could lead to the efficient delivery of PI. After filling the underlying microfluidic channel with 0.1 mg/mL PI dye, 200 pulses of 20 V with 200 μs duration time (denoted as 20 V/200 μs/200 pulses) were applied,

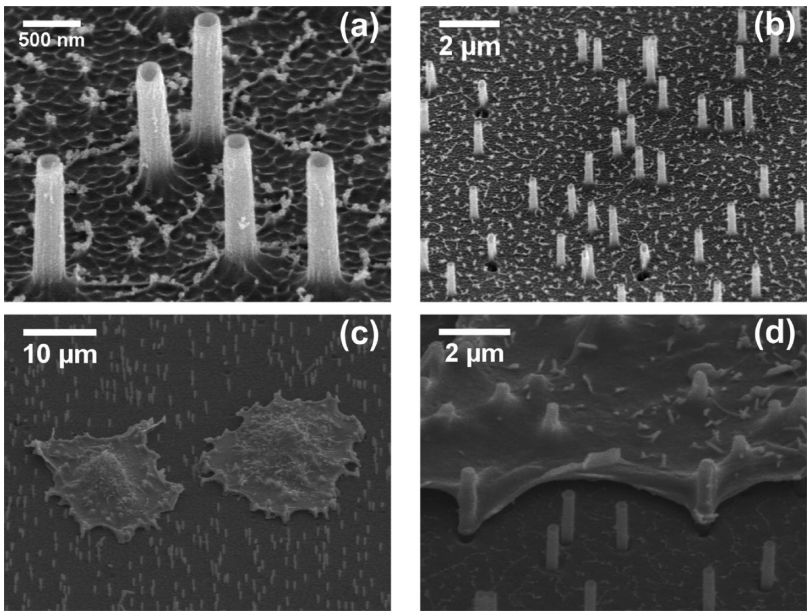

Figure 2. Cells cultured on nanostraws. (a, b) SEM images of nanostraw membranes. Typically the nanostraws have a diameter of 250 nm and the nanostraw array density is about 0.2 straws/μm^2. (c) False color SEM images of CHO cells cultured on nanostraw membrane for 24 h and (d) close cell membrane−nanostraw interfaces.

followed by a 5 min waiting period to allow PI dye to enter the cell. To avoid signal artifacts through nonspecific cellular uptake and absorption of PI dye, the fluidic channel and cell culture well were each rinsed three times and replaced with new media after the incubation period. Fluorescent microscopy showed that the PI dye was delivered into more than 95% of the cells within 5 min (Figure 3a), and only cells positioned over the microfluidic channel received PI dye (Supporting Information, Figure S3a−c). This spatial selectivity confirms that only local nanoelectroporation occurs rather than bulk electroporation throughout the medium. Cell viability was greater than 95% after the delivery (Figure 3b). The long-term cell viability after electroporation was also evaluated without delivery of PI dye, because PI dye is cytotoxic for cells after 24 h. Results show that the cell viability (98%) three days after electroporation with (20 V/200 μs/200 pulses) were similar compared to cells cultured on nanostraws without electroporation (Supporting Information, Figure S4a,b), demonstrating that nanostraw-mediated electroporation is minimally disruptive. Cell viability remained high even after much stronger electrical pulsing (30 V/200 μs/200 pulses), or 15× dose with 3000 pulses of (20 V/200 μs; Figure 3c), suggesting the typical electroporation conditions were not general cytotoxic.

We next examined whether nanostraw-mediated electroporation could deliver larger biochemically active molecules such as plasmids without disrupting normal cell function. Similar to the PI experiments, after introducing 0.08 μg/μL of a pRFP into the microfluidic channel, applying (20 V/200 μs/200 pulses), and allowing 24 h for DNA expression, 81% of CHO cells showed positive pRFP transfection signals (Figure 3d), with a cell viability of 98%. HEK 293 cells were also successfully transfected with an efficiency of 67% by applying similar plasmid concentrations and pulsing conditions used for the transfecting CHO cells (Supporting Information, Figure S5a).

To assess the specificity of our nanostraw device, we conducted experiments on cells cultured on 250 nm nanostraw membranes without electroporation. The results showed that a 250 nm nanostraw device without electroporation was neither able to deliver PI dye into cells (Supporting Information, Figure S5b) nor able to transfect cells with pRFP (Figure 3e), even with plasmid concentrations 10-fold higher (1 μg/μL). As a further control, we also attempted electroporation of cells cultured on the nanoporous membranes but without nanostraws. Intriguingly, electroporation through the porous membranes was capable of delivering PI dye into cells with moderate yield (Supporting Information, Figure S5c) but pRFP transfection efficiency was less than 20% (Figure 3f). The much larger molecular weight of the plasmid (~5000 bp construct, 3×10^6 Da) compared to PI dye (molecule weight ~ 700 Da) and the resulting lower diffusion rate may explain this observation. Even with higher voltages (60 V/200 μs/200 pulses), longer pulses (20 V/2 ms/200 pulses), or higher plasmid concentration (0.5 μg/μL), no transfection efficiencies greater than 40% were observed, while cell viability decreased rapidly. These experiments suggest that the close interface between cell membranes and nanostraws is the key for effective and safe electroporation.

Although a moderate voltage (20 V/200 μs/200 pulses) was used for most experiments, lower voltages and shorter duration pulses (6 V/20 μs/2000 pulses) were also sufficient to achieve successful pRFP transfection (71%)

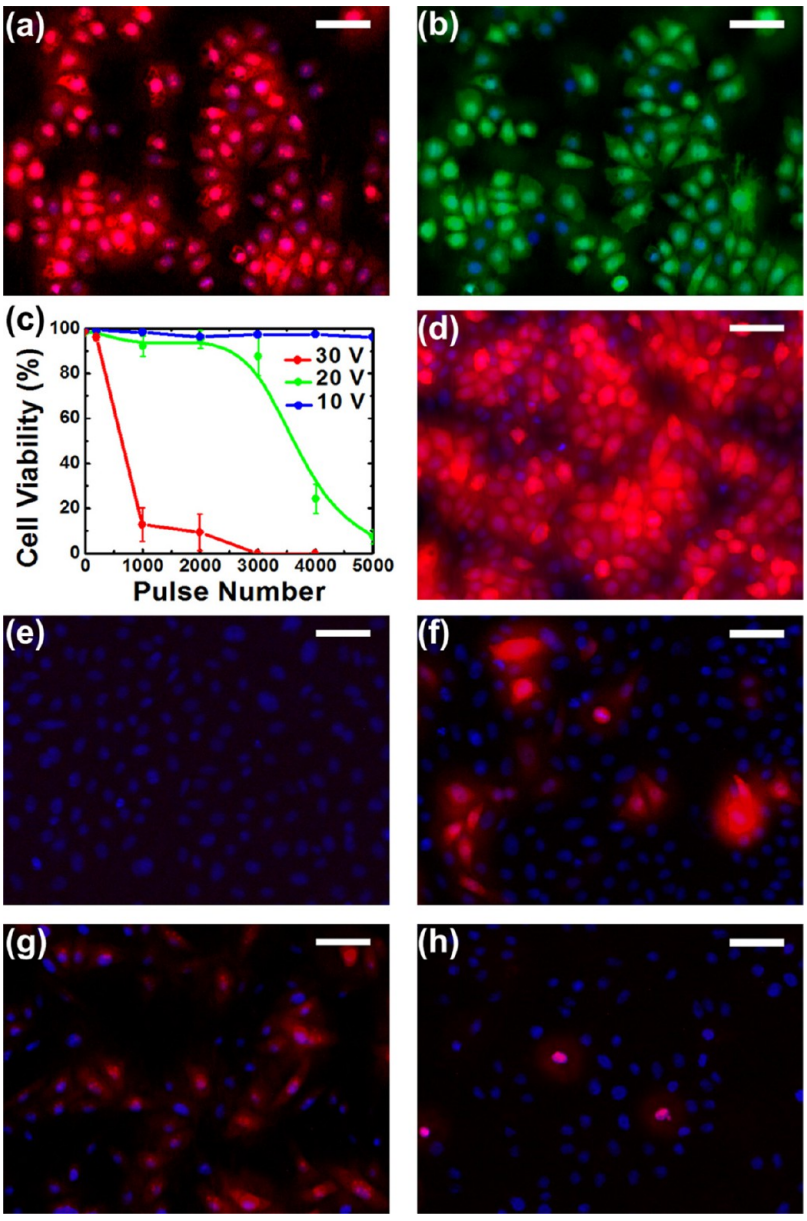

Figure 3. PI delivery and pRFP transfection. (a. b) Delivery of PI dye (red) into live CHO cells (green) with >95% efficiency. (c) Cell viability in 3 days after electroporation at different pulse numbers and voltages was evaluated (pulse duration time: 200 μm; frequency: 20 Hz). (d) pRFP transfection with high efficiency. A total of 81% of CHO cells showed positive pRFP transfection (red) after 24 h. (e) No pRFP transfection was observed when using nanostraws without electroporation. (f) Localized electroporation with porous membranes without nanostraws yielded a low efficiency of pRFP transfection (<20%). (g) Adding PI dye 10 s after electroporation yielded positive delivery signals, while (h) adding PI dye 10 min after electroporation resulted in no PI delivered, which confirmed cell membrane resealing within 10 min after electroporation. In (a–h), cell nuclei were labeled with hoechst 33342 (blue) to facilitate identification. Scale bar: 50 μm.

to CHO cells using nanostraw-electroporation (Supporting Information, Figure S5d), while electroporation using a flat porous substrate failed to show any transfection signals. The trade-off between delivery efficiency and cell viability is thus not that severe over a range of voltages as a result of the more intimate contact between the cell membrane and the nanostraw.

The formation of transient cell membrane pores after electroporation followed by self-healing is highly preferable for intracellular delivery.[11] We hypothesized that our nanostraw–electroporation system would serve as a "valve", opening transient pores during poration, followed by membrane resealing after removal of the voltage. Several recent experiments using electroporation for electrophysiological measurements have observed similar phenomena.[12,27,28] We tested this concept by assessing whether PI dye, added into the microfluidic channel 10 s or 10 min after electroporation was also delivered into CHO cells. In accordance with this hypothesis, delivery of PI 10 s after electroporation produced a significant level of red fluorescence (Figure 3g), while delivery after 10 min failed to show

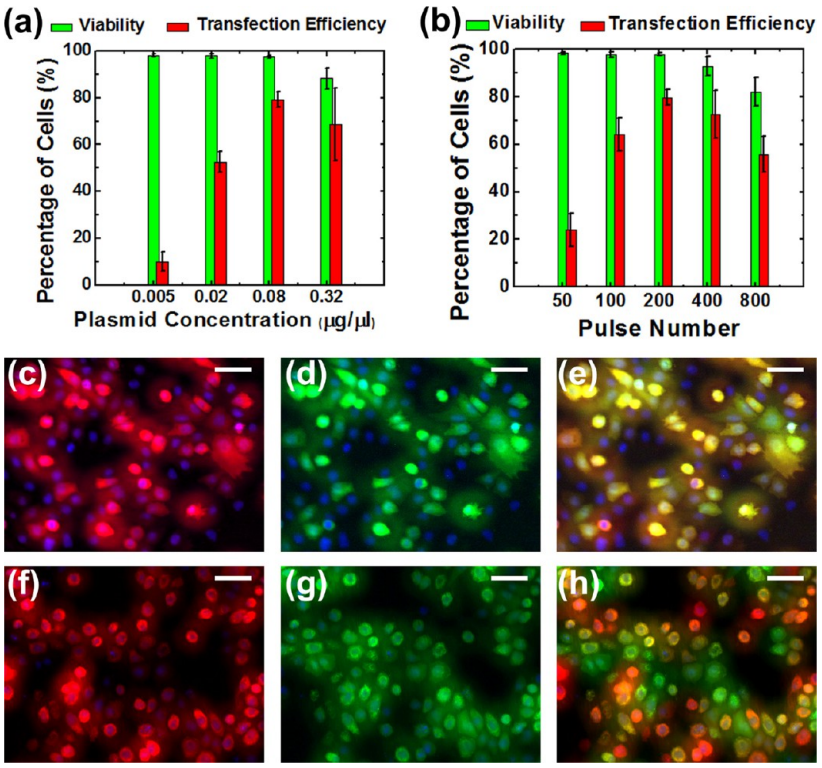

Figure 4. Dose control, cotransfection, and sequential transfection. pRFP transfection efficiency and cell viability controlled by (a) plasmid concentration and (b) pulse number. (c−e) Simultaneous transfection of (c) pRFP (red) and (d) pGFP (green) into the same cells with high efficiency. (e) Merged image demonstrating colocalization of RFP and GFP. (f−h) Sequential transfection of (f) pRFP (red) and (g) pGFP (green) with a 24 h interval. (h) Merged images show simultaneous RFP and GFP expression (74%), although their intensities are uncorrelated. In (c−h), cell nuclei were labeled with hoechst 33342 (blue) to facilitate identification. Scale bar: 50 μm.

any fluorescence (Figure 3h). Similar results were observed on delivery of pRFP (Supporting Information, Figure S5e,f), confirming that in this system, the cell membrane reseals within 10 min after electroporation.

In experiments where the PI dye or plasmid was introduced even 10 s after electroporation, the efficiency and fluorescence level of delivered PI dye or pRFP transfection was much lower compared to experiments where PI and plasmid were present during electroporation, suggesting either rapid membrane closure or electrokinetic delivery during poration. Indeed, transfection efficiency decreased dramatically if electrode polarity was reversed during electroporation (Supporting Information, Figure S6a−c). These observations suggest that the electric field not only plays an essential role for cell membrane penetration, but assists in the transport of biomolecules.

In addition to excellent capabilities for spatial and temporal control, we were keen to explore whether nanostraw-mediated electroporation could also be used to control plasmid dosage and expression levels. This was examined by adjusting the concentration of added plasmid (Figure 4a) or the number of applied pulses (Figure 4b). Here, we assessed the dose−response relationship of transfection efficiency (number of transfected cells) and cell viability, as well as gene expression level (by measuring RFP fluorescent intensity), in terms of plasmid concentration used and the number of pulses applied. At (20 V/200 μs), as concentration increased from 0 to 0.08 μg/μL, or pulse number increased from 0 to 200, transfection efficiency increased in a monotonic manner 24 h post electroporation, implying that nanostraw electroporation can be used to deliver a controlled and reasonably uniform amount of genetic material. However, the toxicity of DNA at higher dose limited cellular viability[29] and by extension, transfection efficiency. Gene expression levels and cell viability 3 days after transfection were evaluated as well (Supporting Information, Figure S7a,b). High cell viability after transfection was maintained at low gene expression level when a low dose of plasmid (<0.08 μg/μL or <400 pulses) was delivered. However, at higher doses, gene overexpression leads to low cell viability after transfection (Supporting Information, Figure S7c,d).

Techniques for cotransfection of two or more DNA plasmid or RNA are critical when the simultaneous expression of several genes is needed.[30−32] However, 1:1 cotransfection to the same recipient cell is challenging with conventional techniques (lipofectamine, viral delivery, bulk electroporation) due to their stochastic nature.[33] We thus evaluated whether cells can be efficiently cotransfected with two different plasmids, one encoding RFP and a second green fluorescent protein (pGFP; Figure 4c−e). The fluorescent intensities of GFP and RFP inside each cell were highly

correlated with each other, showing that both plasmids were delivered in equal quantities into each single cell (Supporting Information, Figure S8a).

Sequential transfection is also important when periodic transfection is required, or when the knockdown of pre-expressed signals is needed.[31,34,35] However, a high degree of sequential transfection efficiency is very difficult to achieve with most traditional techniques.[33] To determine the potential of our system as a tool for sequential transfection, we evaluated the delivery of pRFP and pGFP to the same cells within a 24 h interval. After 24 h of further incubation, 74% of the cells coexpressed RFP and GFP (Figure 4f–h). The fluorescent intensity of RFP and GFP in the same cell was uncorrelated (Supporting Information, Figure S8b) showing cell access over this time period consisted of two independent events.

The nanostraw membranes can be easily implemented for biological use based on their simple architecture and fabrication. For example, the nanostraw membrane can combined with commercial transwell-style dishes, which can be inserted into typical cell culture dishes with an accompanying ITO disk. Perhaps, most importantly, a large quantity of cells can be transfected in parallel with uniform results, allowing facile transformation on a simple Petri-style dish. Currently it is difficult to clean and reuse these devices, however, given the inexpensive nature of a single device, this does not appear necessary.

CONCLUSION

In summary, nanostraw devices can be used as a practical, safe, and effective electroporation system. Low-voltage electric pulses are sufficient to serve as a valve, enabling transient access into the cytosol. This system successfully delivers membrane-impermeable dyes and plasmids in a parallel fashion over large areas, while maintaining high cell viability. Highly effective cotransfection and sequential transfection were also demonstrated, which are difficult to achieve with conventional delivery methods. In addition to the delivery of plasmid and dye molecules shown in this work, the system can be easily extended to deliver other biomolecules, such as peptides, RNA, and proteins, and the required amount of biochemical may be reduced because the electroporated region is coincident with the reagents delivered from the nanostraws. The platform itself is highly practical and can be easily produced in large quantities. Studies with additional cell types are necessary to prove the universality of cellular transfection with this method, yet the success of other nanowire systems on diverse cell types is highly encouraging.

METHODS

Fabrication. Nanostraw membrane fabrication: track-etched polycarbonate membrane (Maine Manufacturing, 2×10^7 pores/cm^2 and pore size 250 nm) were coated with alumina by atomic layer deposition (ALD, TMA, H_2O, Cambridge Nanotech) using the well-established trimethyl-aluminum ($AlMe_3/H_2O$) ALD process. To achieve conformal coverage over high aspect ratio nanopores, pulse cycles of 0.015 s (precursor exposure time), 60 s (time that precursors were retained in the ALD chamber), and 60 s (N_2 purge time) were used for both $AlMe_3$ and H_2O pulses. Normally 100 pulse cycles give 20 nm thick Al_2O_3 film. In the second step, alumina on the top surface of polycarbonate membrane was selectively etched with a gas flow composition of 30 sccm Cl_2, 40 sccm BCl_3, and 5 sccm Ar at ECR 300 W and RF 60 W. In the third step, polycarbonate membrane was selectively etched with 30 sccm O_2 at ECR 200 W and RF 60 W to expose the alumina straw.

Microfluidic Assembly and Device Making. Microfluidic devices were prepared with PDMS elastomer and cross-linker (Sylgard 184, Dow Corning). Before device assembly, nanostraw membranes and PDMS layers were treated with oxygen plasma at 100 W for 20 s. Immediately after plasma treatment, the bottom PDMS layer which contained the microfluidic channel was placed on top of a ITO-coated glass slide. The nanostraw membrane was placed over the microfluidic channel, and the PDMS layers were pressed together and cured at 95 °C for 30 min to complete PDMS assembly. To prepare devices for cell culture, the microfluidic devices were sterilized with UV light for 30 min, followed by overnight incubation with poly-D-lysine solution before cell plating.

Cell Culture. CHO-K1, Human Embryonic Kidney 293T cells (HEK 293) were cultured in DMEM supplemented with 10% fetal bovine serum and 1% antibiotics at 37 °C and 5% CO_2. Normally cells were cultured for 12–24 h before electroporation and delivery experiments.

SEM. Samples were characterized using SEM. For cell samples, specimens were prepared by Critical Point Dry (CPD) process before imaging. Typically samples were rinsed with PBS and then fixated with 2% glutaraldehyde solution for 30 min, followed by 3 washes in cacodylate buffer at pH 7.4. The cells were then labeled with osmium tetroxide in order to improve contrast, then gradually transferred to ethanol, and finally critical point dried. Samples were sputter-coated with gold–palladium and imaged in SEM.

Plasmid. The pmCherry-C1 plasmid (Clontech) encoding for Red Fluorescent Protein (RFP), and the pEGFP-C1 plasmid encoding for the enhanced green fluorescent protein (EGFP) (Clontech) were propagated in competent NEB 10-Beta competent *Escherichia coli*. The plasmid was extracted and purified using the PureLink HiPure Plasmid Filter Maxiprep Kit (Invitrogen). Plasmids were dissolved with distilled water.

Electroporation and Delivery. PI dye delivery: platinum electrode was placed in the cell medium serving as cathode and ITO glass underneath microfluidic channel served as anode. 0.1 mg/mL PI dye (dissolved in PBS) was injected into the microfluidic channel. Pulses of (20 V/200 μs/20 Hz/200 pulses) were then applied, followed by incubation at 37 °C for 5 min to allow the entering of PI dye into cells. After that, cell medium was replaced with new medium and microfluidic channel was rinsed with PBS three times before imaging.

Plasmid transfection: platinum electrode was placed in the cell medium serving as anode and ITO glass underneath microfluidic channel served as cathode. Typically, 0.01–0.3 μg/μL plasmid (dissolved in DI water) was injected into the microfluidic channel. Pulses of 20 V/200 μs/20 Hz/200 pulses were then applied. After 1 h, plasmid solution in microfluidic channel was replaced with fresh medium. Cells were incubated for 24–72 h for gene expression.

For cell viability experiments, cells were stained with hoechst 33342 to label all the cell nucleus and stained with calcein AM to label all the live cells. In some experiments, ethidium homodimer was used to label dead cells. Transfection efficiency was calculated by counting the number percentage

of positive transfected cells over the total cells (including both live and dead cells).

For low voltage electroporation/transfection experiment, most of procedures were the same except that the applied pulse used 6 V/20 μs/20 Hz/2000 pulses. At this 6 V and 20 μs electroporation condition, cells can survive for $\gg$2000 pulses. For cotransfection experiment, 0.05 μg/μL RFP plasmid and 0.05 μg/μL GFP plasmid were added into the microfluidic channel at the same time, followed by electroporation. For sequential transfection experiment, cells were electroporated and with 0.05 μg/μL pRFP on the first day, followed by second electroporation and transfection with 0.05 μg/μL pGFP on the second day. Cells were incubated for another 24 h for gene expressing.

Microscopy. Axiovert 200 M platform (Zeiss) with filter sets 10 and 0 (Zeiss) and Ex120 light source (X-cite) were used to take the epifluorescence microscope images.

Conflict of Interest: The authors declare no competing financial interest.

Supporting Information Available: Supplemental figures. This material is available free of charge *via* the Internet at http://pubs.acs.org.

Acknowledgment. The authors wish to thank the Yi Cui and Sarah Heilshorn laboratories for use of equipment and experimental advice. This work was supported by the National Institutes of Health Grant R21 MH091471 (C.C.G.), the United States Israel Binational Science Foundation Grant 2007425 (C.C.G.), the Coulter Foundation (N.M. and C.C.G.), and a Stanford BioX-Neuroventures Award (N.M. and C.C.G.). X.X. acknowledges the China Scholarship Council (File No. 2009638027) and NSF NSEC Center for Probing the Nanoscale for support. A.X. acknowledges the NSF graduate fellowship for support.

REFERENCES AND NOTES

1. Cai, D.; Mataraza, J. M.; Qin, Z.-H.; Huang, Z.; Huang, J.; Chiles, T. C.; Carnahan, D.; Kempa, K.; Ren, Z. Highly Efficient Molecular Delivery into Mammalian Cells Using Carbon Nanotube Spearing. *Nat. Methods* **2005**, *2*, 449–454.
2. Gu, Z.; Biswas, A.; Zhao, M.; Tang, Y. Tailoring Nanocarriers for Intracellular Protein Delivery. *Chem. Soc. Rev.* **2011**, *40*, 3638.
3. Luo, D.; Saltzman, M. Synthetic DNA Delivery Systems. *Nat. Biotechnol.* **1999**, *18*, 33–37.
4. Pack, D. W.; Hoffman, A. S.; Pun, S.; Stayton, P. S. Design and Development of Polymers for Gene Delivery. *Nat. Rev. Drug Discovery* **2005**, *4*, 581–593.
5. Xu, Y.; Francis, C.; Szoka, J. Mechanism of DNA Release from Cationic Liposome/DNA Complexes Used in Cell Transfection. *Biochemistry* **1996**, *35*, 5616–5623.
6. Merdana, T.; Kopecekb, J.; Kissela, T. Prospects for Cationic Polymers in Gene and Oligonucleotide Therapy against Cancer. *Adv. Drug Delivery Rev.* **2002**, *54*, 715–758.
7. Stephens, D. J. The Many Ways to Cross the Plasma Membrane. *Proc. Natl. Acad. Sci. U.S.A.* **2001**, *98*, 4295–4298.
8. Kay, M. A.; Glorioso, J. C.; Naldini, L. Viral Vectors for Gene Therapy: The Art of Turning Infectious Agents into Vehicles of Therapeutics. *Nat. Med.* **2001**, *7*, 33–40.
9. Wong, I. Y.; Almquist, B. D.; Melosh, N. A. Dynamic Actuation Using Nano-Bio Interfaces. *Mater. Today* **2010**, *13*, 14–22.
10. Adler, A. F.; Leong, K. W. Emerging Links between Surface Nanotechnology and Endocytosis: Impact on Nonviral Gene Delivery. *Nano Today* **2010**, *5*, 553–569.
11. Gehl, J. Review: Electroporation: Theory and Methods, Perspectives for Drug Delivery, Gene Therapy and Research. *Acta Physiol. Scand.* **2003**, *177*, 437–447.
12. Golzio, M. Direct Visualization at the Single-Cell Level of Electrically Mediated Gene Delivery. *Proc. Natl. Acad. Sci. U. S.A.* **2002**, *99*, 1292–1297.
13. Boukany, P. E.; Morss, A.; Liao, W.; Henslee, B.; Jung, H.; Zhang, X.; Yu, B.; Wang, X.; Wu, Y.; Li, L.; et al. Nanochannel Electroporation Delivers Precise Amounts of Biomolecules into Living Cells. *Nat. Nanotechnol.* **2011**, *6*, 747–754.
14. Khine, M.; Lau, A.; Ionescu-Zanetti, C.; Seo, J.; Lee, L. P. A Single Cell Electroporation Chip. *Lab Chip* **2005**, *5*, 38.
15. Guignet, E. G.; Meyer, T. Suspended-Drop Electroporation for High-Throughput Delivery of Biomolecules into Cells. *Nat. Methods* **2008**, *5*, 393–395.
16. Canatella, P. J.; Karr, J. F.; Petros, J. A.; Prausnitz, M. R. Quantitative Study of Electroporation-Mediated Molecular Uptake and Cell Viability. *Biophys. J.* **2001**, *80*, 755–764.
17. Fei, Z.; Wang, S.; Xie, Y.; Henslee, B. E.; Koh, C. G.; Lee, L. J. Gene Transfection of Mammalian Cells Using Membrane Sandwich Electroporation. *Anal. Chem.* **2007**, *79*, 5719–5722.
18. Fei, Z.; Hu, X.; Choi, H.-w.; Wang, S.; Farson, D.; Lee, L. J. Micronozzle Array Enhanced Sandwich Electroporation of Embryonic Stem Cells. *Anal. Chem.* **2010**, *82*, 353–358.
19. Ishibashi, T.; Takoh, K.; Kaji, H.; Abe, T.; Nishizawa, M. A Porous Membrane-Based Culture Substrate for Localized *In Situ* Electroporation of Adherent Mammalian Cells. *Sens. Actuators, B* **2007**, *128*, 5–11.
20. Shalek, A. K.; Robinson, J. T.; Karp, E. S.; Lee, J. S.; Ahn, D. R.; Yoon, M. H.; Sutton, A.; Jorgolli, M.; Gertner, R. S.; Gujral, T. S.; et al. Vertical Silicon Nanowires as a Universal Platform for Delivering Biomolecules into Living Cells. *Proc. Natl. Acad. Sci. U.S.A.* **2010**, *107*, 1870–1875.
21. Shalek, A. K.; Gaublomme, J. T.; Wang, L.; Yosef, N.; Chevrier, N.; Andersen, M. S.; Robinson, J. T.; Pochet, N.; Neuberg, D.; Gertner, R. S.; et al. Nanowire-Mediated Delivery Enables Functional Interrogation of Primary Immune Cells: Application to the Analysis of Chronic Lymphocytic Leukemia. *Nano Lett.* **2012**, *12*, 6498–6504.
22. Park, S.; Kim, Y.-S.; Kim, W. B.; Jon, S. Carbon Nanosyringe Array as a Platform for Intracellular Delivery. *Nano Lett.* **2009**, *9*, 1325–1329.
23. Kim, W.; Ng, J. K.; Kunitake, M. E.; Conklin, B. R.; Yang, P. Interfacing Silicon Nanowires with Mammalian Cells. *J. Am. Chem. Soc.* **2007**, *129*, 7228–7229.
24. Hanson, L.; Lin, Z. C.; Xie, C.; Cui, Y.; Cui, B. Characterization of the Cell−Nanopillar Interface by Transmission Electron Microscopy. *Nano Lett.* **2012**, *12*, 5815–5820.
25. Berthing, T.; Bonde, S.; Rostgaard, K. R.; Madsen, M. H.; Sørensen, C. B.; Nygård, J.; Martinez, K. L. Cell Membrane Conformation at Vertical Nanowire Array Interface Revealed by Fluorescence Imaging. *Nanotechnology* **2012**, *23*, 415102.
26. VanDersarl, J. J.; Xu, A. M.; Melosh, N. A. Nanostraws for Direct Fluidic Intracellular Access. *Nano Lett.* **2012**, *12*, 3881–3886.
27. Xie, C.; Lin, Z.; Hanson, L.; Cui, Y.; Cui, B. Intracellular Recording of Action Potentials by Nanopillar Electroporation. *Nat. Nanotechnol.* **2012**, *7*, 185–190.
28. Robinson, J. T.; Jorgolli, M.; Shalek, A. K.; Yoon, M.-H.; Gertner, R. S.; Park, H. Vertical Nanowire Electrode Arrays as a Scalable Platform for Intracellular Interfacing to Neuronal Circuits. *Nat. Nanotechnol.* **2012**, *7*, 180–184.
29. Chu, G.; Hayakawa, H.; Berg, P. Electroporation for the Efficient Transfecdon of Mammalian Cells with DNA. *Nucleic Acids Res.* **1987**, *15*, 1311–1326.
30. Sankpal, N. V.; Fleming, T. P.; Gillanders, W. E. Dual Expression Lentiviral Vectors for Concurrent RNA Interference and Rescue. *J. Surg. Res.* **2009**, *156*, 50–56.
31. Xu, X.-M.; Yoo, M.-H.; Carlson, B. A.; Gladyshev, V. N.; Hatfield, D. L. Simultaneous Knockdown of the Expression of Two Genes Using Multiple shRNAs and Subsequent Knock-In of Their Expression. *Nat. Protoc.* **2009**, *4*, 1338–1348.
32. D'Ovidio, F.; Daddi, N.; Suda, T.; Grapperhaus, K.; Patterson, A. G. Efficient Naked Plasmid Cotransfection of Lung Grafts by Extended Lung/Plasmid Exposure Time. *Ann. Thorac. Surg.* **2001**, *71*, 1817–1824.
33. Xie, Z. L.; Shao, S. L.; Lv, J. W.; Wang, C. H.; Yuan, C. Z.; Zhang, W. W.; Xu, X. J. Co-Transfection and Tandem Transfection of HEK293A Cells for Overexpression and RNAi Experiments. *Cell Biol. Int.* **2011**, *35*, 187–192.

34. Dong, X. W.; Goregoaker, S.; Engler, H.; Zhou, X.; Mark, L.; Crona, J.; Terry, R.; Hunter, J.; Priestley, T. Small Interfering RNA-Mediated Selective Knockdown of NaV1.8 Tetrodotoxin-Resistant Sodium Channel Reverses Mechanical Allodynia in Neuropathic Rats. *Neuroscience* **2007**, *146*, 812–821.
35. Jiang, Y.; Price, D. Rescue of the TTF2 Knockdown Phenotype with an siRNA-Resistant Replacement Vector. *Cell Cycle* **2004**, *3*, 1151–1153.